X-RAY PHOTOELECTRON SPECTROSCOPIC (XPS) STUDIES OF CLEAN AND ION BEAM BOMBARDED Sb_2Te_2Se AND $(Bi_{0.7}Sb_{0.3})_2Se_{3.0}$ (111) SURFACES

Zdenek BASTL[1], Ilona SPIROVOVA and Michaela JANOVSKA

J. Heyrovsky Institute of Physical Chemistry, Academy of Sciences of the Czech Republic, 182 23 Prague 8, Czech Republic; e-mail: [1] bastl@jh-inst.cas.cz

Received October 3, 1996
Accepted October 18, 1996

Dedicated to Dr Karel Mach on the occasion of his 60th birthday.

The first detailed study of photoelectron spectra of Sb_2Te_2Se and $(Bi_{0.7}Sb_{0.3})_2Se_3$ (111) clean and sputtered surfaces is presented as part of an XPS examination of the surface chemistry of these and related materials. The core level binding energies and surface chemical composition have been determined from the XPS data. On substitution of Te by Se in Sb_2Te_3 leading to Sb_2Te_2Se the core level binding energies in Sb and Te increase by 0.3 eV while in Bi_2Se_3 the binding energy of core electrons does not change on replacement of Bi by Sb. The measured core level shifts are caused by changes of the initial state charge distribution and result in increase of average ionicity of bonding in the Sb_2Te_2Se crystal. The surface composition of Sb_2Te_2Se sample calculated from intensities of photoelectron spectra agrees well with the bulk composition of the crystal while $(Bi_{0.7}Sb_{0.3})_2Se_3$ sample shows enrichment in Bi. The effect of argon ion bombardment on surface composition for various impact conditions has been investigated. The surface enrichment in Sb and Bi for Sb_2Te_2Se and $(Bi_{0.7}Sb_{0.3})_2Se_3$ sample due to different atomic sputtering yields is observed. It follows from the relative intensities of photoelectron spectra measured at different detection angles that the ordered arrangement of the superficial layers sampled by the XPS method is damaged by sputtering at ion energies as low as 200 eV and doses $I > 2 \cdot 10^{15}$ ion/cm^2.

Key words: X-Ray photoelectron spectroscopy; Substitution effects; Ion sputtering; $Sb_2Te_{3-x}Se_x$; $(Bi_{1-x}Sb_x)_2Se_3$.

The narrow bandgap (≈0.1 eV) $A_2^VB_3^{VI}$ mixed semiconductors with a rhombohedral lattice are attracting much attention as promising materials for thermoelectric applications[1]. The crystal lattice of these semiconductors[2] is formed by periodic arrangements of layers perpendicular to the trigonal axis *c*. Each layer is composed of five atomic planes arranged according to the pattern …B^1-A-B^2-A-B^1… (see Fig. 1). There is a van der Waals gap between B^1 atomic planes of adjacent layers. Due to the predominantly van der Waals nature of interlayer bonds the (111) cleavage plane is well defined, atomically smooth and unreconstructed. Interest in the $Sb_2Te_{3-x}Se_x$ (x = 0 to 1) and $(Bi_{1-x}Sb_x)_2Se_3$ (x = 0 to 1) ternary systems has increased during the last decade, because their transport and thermoelectric properties can be varied by changing elemental com-

position. While exhaustive literature[1,3–8] is available on preparation, optical and electrical transport properties of these materials, systematic studies on the effects of substitution on charge distribution are rather scarce. For applications also the thermal and electrical reliability of the contact between the thermoelectric material and the metal electrode is of considerable importance. Many standard contact methods cause a deterioration of the thermoelectric and mechanical properties by diffusion of the contact electrode material and other surface impurities[9]. For cleaning of surfaces their irradiation with ion beams is widely used in surface science and technology. However, it is well established that many physical and chemical properties of surfaces may be modified by the ion beams[10–12]. The surface may be etched by physical sputtering or chemical reaction, this film may be deposited on the surface, or grown from chemical reactions between the incident particles and the surface[13–14]. Energy may be transferred between the colliding particles and the surface, leading in some cases to the emission of light or electrons. The rates at which these various processes occur depend primarily on the velocity of the incident particle, frequently increasing greatly as the incident energy increases. For low energy of incident ions the sputtered ions are emitted from within 1–2 atomic layers. In spite of a large amount of data and knowledge obtained on the ion-solid interaction a detailed description of surface modifications is still missing. In addition, extrapolation of the available results to other experimental conditions and materials is not always possible. At low ion energies atomic mixing and amorphization consisting in rearrangement of the atoms due to interaction with ions are important processes. The layered materials with well defined in-depth distribution of elements are well suited for the study of ion damaging processes.

X-Ray photoelectron spectroscopy (XPS) is a surface sensitive method with typical information depth of 1–5 nm, giving in one experiment definite information on the chemical composition and electron density distribution in the superficial layers of ma-

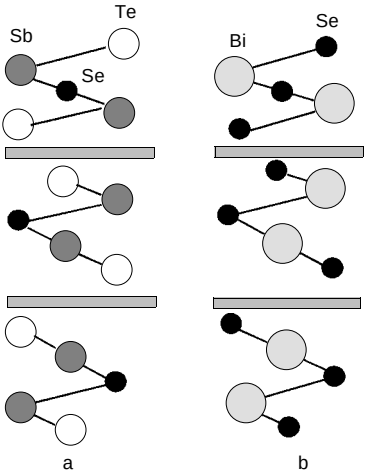

FIG. 1
Structure of : (a) Sb_2Te_2Se and (b) Bi_2Se_3 along the *c* axis, projected on the *a–c* plane

terials. The method allows to perform quantitative analysis with a relative precision up to 5%. In this work we have used the XPS method to evaluate the changes of atomic charges accompanying the substitution of Te by Se in Sb_2Te_3 and Bi by Sb in Bi_2Se_3. Furthermore, we have also investigated the changes of surface composition caused by bombardment of Sb_2Te_2Se and $(Bi_{0.7}Sb_{0.3})_2Se_{3.0}$ (111) surfaces by argon ions with low (200–400 eV) and high (≈5 keV) energies. The question raised in this paper are: How is the surface composition modified by ion irradiation? What are the conditions for the least damaging bombardment? Is there an energy threshold for ion damage? The ability of the XPS technique to determine the surface composition and to distinguish between the different chemical states of elements makes this method very efficient in study of these changes.

EXPERIMENTAL

Sb_2Te_2Se and $(Bi_{0.7}Sb_{0.3})_2Se_{3.0}$ as well as parent Sb_2Te_3 and Bi_2Se_3 single crystals were obtained from Department of General and Inorganic Chemistry, University of Pardubice (Czech Republic). The latter two samples were studied for comparative purposes. The crystals were prepared from elements of 99.999% purity. They were grown using vertical Bridgman method. A clean surface was prepared by cleaving the crystal along (111) plane under ultrahigh vacuum (≈10^{-8} Pa) in preparation chamber of the electron spectrometer. Ion irradiation of Sb_2Te_2Se and $(Bi_{0.7}Sb_{0.3})_2Se_{3.0}$ (111) surfaces was performed using an Ar^+ ion beams produced by VG AG1 (200–500 eV) and AG2 (2–10 keV) ion sources.

Electron spectra were measured using a VG ESCA 3 Mk II spectrometer equipped with twin anode X-ray source (AlKα/MgKα). The vacuum in the spectrometer was typically 3 . 10^{-8} Pa. The electron energy resolution defined as the width (FWHM) of the Au $4f_{7/2}$ line (binding energy 84.0 eV) was 1.2 eV. The electron energies were measured with respect to the Fermi level. The Se 3d, Sb 4d, Te 4d, Bi 5d and valence band (in some experiments also Sb 3d, Te 3d, Bi 4f and selected Auger transitions) photoelectron spectra were measured at high resolution and at several (at least two) different take-off angles. At lower detection angles (with respect to the sample surface) the surface selectivity of the method is increased. In order to increase the signal to noise ratio, repeated scans and data summing were made. Data acquisition and processing were performed using routine programs. The Shirley-type[15] non-linear background was used. The overlapping peaks were resolved into individual components using the lines of Gaussian–Lorentzian shape and the damped non-linear least square technique[16]. Theoretical photoionization cross-sections[17] were used to convert peak areas into the elemental concentrations.

RESULTS AND DISCUSSION

Clean Surfaces

The survey spectra (Fig. 2) of Sb_2Te_3, Sb_2Te_2Se, Bi_2Se_3 and $(Bi_{0.7}Sb_{0.3})_2Se_3$ (111) surfaces have shown no peaks which could be attributed to contaminations demonstrating thus the cleanliness of the studied surfaces. The core level binding energies as well as the photoemission peak widths at half heights (FWHM) are listed in Table I. Spin-orbit

splitting of the Se 3d level is not clearly observed. For Bi_2Se_3 sample the obtained binding energies are in very good agreement with the previously reported values[18–20]. The structure of Sb_2Te_3 and Bi_2Se_3 (Fig. 1) implies the existence of two types of inequivalent group VI atoms in the lattice. However, the photoelectron spectra show no evidence of the two distinct peaks. This result indicates that in spite of the difference in bonding environment the difference in the atomic charges between $Te^1(Se^1)$ and

TABLE I
The core level binding energies, E_B, and widths, FWHM, of the photoemission lines (in parentheses). All data are in eV

Sample	E_B						
	Sb $4d_{5/2}$	Sb $3d_{5/2}$	Te $4d_{5/2}$	Te $3d_{5/2}$	Bi $5d_{5/2}$	Bi $4f_{7/2}$	Se 3d
Sb_2Te_3	32.5	528.6	39.8	572.3	–	–	–
	(1.3)	(1.4)	(1.4)	(1.4)			
Sb_2Te_2Se	32.8	530.0	40.1	572.5	–	–	54.0
	(1.3)	(1.4)	(1.3)	(1.4)			(1.8)
Bi_2Se_3	–	–	–	–	24.8	157.9	53.7
					(1.3)	(1.1)	(1.7)
$(Bi_{0.7}Sb_{0.3})_2Se_3$	32.8	529.0	–	–	24.8	157.8	53.7
	(1.3)	(1.4)			(1.2)	(1.2)	(1.8)

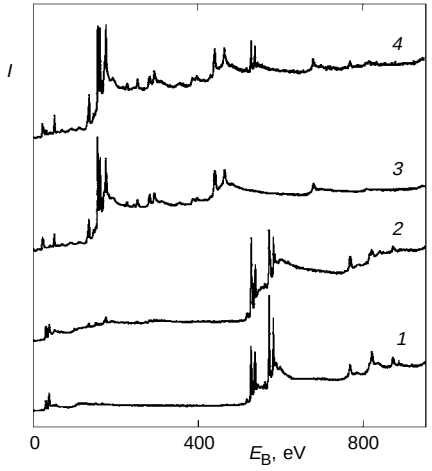

FIG. 2
The XPS wide-scan survey spectra of (111) cleaved surfaces of: (*1*) Sb_2Te_3, (*2*) Sb_2Te_2Se, (*3*) Bi_2Se_3, (*4*) $(Bi_{0.7}Sb_{0.3})_2Se_3$

$Te^2(Se^2)$ atoms is rather small or is compensated by the difference in extraatomic relaxation energy. The core level binding energies in both Sb and Te are shifted in Sb_2Te_2Se by 0.3 eV towards higher binding energies compared to Sb_2Te_3. This is consistent with the increase of positive charge on the Sb atom and decrease of negative charge on Te atoms. The shifts show that replacement of Te^2 atoms by more electronegative Se atoms increases the average ionicity of $Sb–Te^2_xSe^2_{1-x}$ bond in the crystal and consequently increase the bond strength and energy gap. It follows from comparison of shifts of the core levels and of Auger peaks[21], accompanying the substitution of Te by Se in Sb_2Te_3, that they are mostly caused by initial state effects, *i.e.* by charge density decrease around Sb and Te atoms. The values of the modified Auger parameters, α (calculated as the sum of Auger electron kinetic energy and photoelectron binding energy[20,22]) for Sb, Te and Se for the samples studied are given in Table II. It follows from the data of this table that the observed variations of α are small and they are within the limits of the experimental error. Taking into account that the changes in modified Auger parameter are principally due to changes in extraatomic relaxation energy we come again to the conclusion that the binding energy shifts are caused by rearrangement of the charge density distribution of the valence electrons on substitution.

On the other hand, electronegativities of Bi and Sb are the same and in accord with this the Bi and Se core level binding energies in Bi_2Se_3 and $(Bi_{0.7}Sb_{0.3})Se_3$ and consequently the atomic charges are identical.

Figure 3 shows the XPS valence band spectra of the samples studied. Their assignment, based on comparison with the spectra of clean surfaces of respective elements is given in Table III. The measured spectra do not differ to much from the spectra generated by superimposing the valence band spectra of the constituent elements. The valence spectrum of Bi_2Se_3 agrees well with that reported in the literature[16,17].

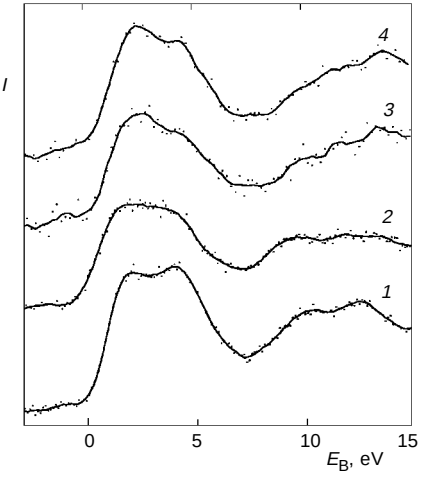

FIG. 3
Valence band photoemission spectra of (*1*) Sb_2Te_3, (*2*) Sb_2Te_2Se, (*3*) Bi_2Se_3, (*4*) $(Bi_{0.7}Sb_{0.3})_2Se_3$ (111) clean surface

For calculation of the stoichiometry of the samples the spectra of electrons emitted at 45° with respect to the sample surface were used. The reason for this is, that as already mentioned at low detection angles the surface selectivity is enhanced and the results are

TABLE II
The modified Auger parameters, α, for the studies samples. All data are in eV

Sample	α		
	Sb	Te	Se
Sb_2Te_3	496.4	532.4	–
Sb_2Te_2Se	496.5	532.5	1 362.8
Bi_2Se_3	–	–	1 362.8
$(Bi_{0.7}Sb_{0.3})_2Se_3$	496.4	–	1 362.7

TABLE III
Binding energies of valence levels, E_B (eV), and their assignment

Sample	E_B	Assignment
Sb_2Te_3	1.6	Te $5p_{3/2}$ + Sb $5p_{3/2}$
	3.9	Te $5p_{1/2}$ + Sb $5p_{1/2}$
	10.0	Sb 5s
	12.7	Te 5s
Sb_2Te_2Se	1.5	Te $5p_{3/2}$ + Sb $5p_{3/2}$
	3.4	Te $5p_{1/2}$ + Sb $5p_{1/2}$ + Se $4p_{3/2}$
	5.1	Se $4p_{1/2}$
	9.9	Sb 5s + Se 4s
	13	Te 5s
Bi_2Se_3	1.9	Bi $6p_{3/2}$
	4.2	Bi $6p_{1/2}$ + Se 4p
	12.5	Bi 6s + Se 4s
$(Bi_{0.7}Sb_{0.3})_2Se_3$	1.8	Bi $6p_{3/2}$ + Sb $5p_{3/2}$
	4.1	Bi $6p_{1/2}$ + Se 4p + Sb $5p_{1/2}$
	12.7	Bi 6s + Se 4s + Sb 5s

influenced by increased contribution of the uppermost layer which is composed of the atoms of one type only. For example, the stoichiometry of the clean $Sb_{2.0}Te_{2.0}Se$ sample measured at detection angle 45°, $Sb_{2.0}Te_{2.0}Se_{0.9}$, is within the experimental error in agreement with the nominal stoichiometry of the sample. The stoichiometry measured at lower detection angle 5°, $Sb_{2.0}Te_{2.14}Se_{0.82}$, is more influenced by the layered structure of the material, …Te–Sb–Se–Sb–Te… (see Fig. 1a), where the uppermost surface layer is composed of tellurium atoms only.

The obtained surface compositions for the samples studied were as follows: $Sb_{2.0}Te_{3.0}$, $Sb_{2.0}Te_{2.0}Se_{0.9}$, $Bi_{2.0}Se_{2.0}$ and $Bi_{2.3}Sb_{0.7}Se_{3.0}$. The stoichiometry of the first two samples agrees within the experimental error with their bulk composition. For samples containing Bi and excess of this element was observed. This overstoichiometry of Bi was found for several different detection angles ranging from 5° to 75° and consequently it can not result from the effects of the photoelectron diffraction. In the core level spectra of the studied samples considerable plasmon-loss peaks are seen (Fig. 4). The inclusion of their intensity into calculation of the surface composition does not lead to stoichiometry different from the results given above. The calculated composition also does not depend on whether Bi 5d and Se 3d or Bi 4f and Se 3s peaks are used for quantitative analysis. It is not the intent of the present paper to discuss the origin of this overstoichiometry in detail. Such discussion would require more experimental data on a series of Bi compounds, which will be reported in a forthcoming study.

Sputtered Surfaces

The surface composition changes when the samples are sputtered by Ar^+ ions. The effect of sputtering on surface composition has been investigated in detail with ternary

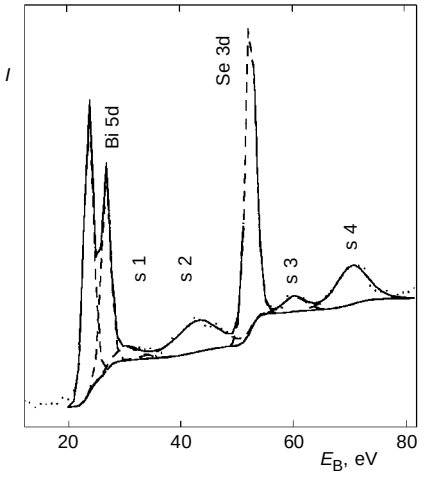

FIG. 4
XPS spectra of Bi 5d and Se 3d electrons in Bi_2Se_3. s1–s4 are energy-loss satellites

samples. Two series of experiments were carried out using Ar^+ ions with low (200 ÷ 400 eV) and high (2.4 ÷ 5 keV) energies, respectively. The employed ion doses ranged from 4 . 10^{14} to 1 . 10^{17} ion/cm^2. Using the angle of incidence (measured from the sample surface) equal to 30° the estimated depth of penetration of ions into the sample is approximately 1–4 nm. The estimated average sputtering rate at low (300 ± 100 eV) ion energies under conditions used in this work is roughly 0.2–0.3 layer/min.

In Fig. 5 the Sb 4d, Te 4d and Se 3d electron spectra of the cleaved unsputtered Sb_2Te_2Se (111) surface along with the spectra of the sputtered surfaces are presented. Sputtering by Ar^+ ions results in gradual surface enrichment in antimony and decrease of tellurium and selenium contents (see Figs 6, 7 and Table IV). The saturation is achieved at ion dose ≈2 . 10^{16} ion/cm^2. In the initial stage of sputtering the selenium concentration (see Table IV) does not change with ion dose monotonously. It increases at low expositions (in the range 0 ÷ 4 . 10^{15} ion/cm^2) while at higher ion doses only decrease was observed. The initial increase in the selenium concentration can be explained as a consequence of a layered structure of the sample (see Fig. 1). Due to this structure the signal from the uppermost Se layer of the unsputtered sample is attenuated by Sb and Te layers present above it and its intensity increases when these two layers are partly removed by sputtering. It follows from the data in Fig. 6 that the ordered

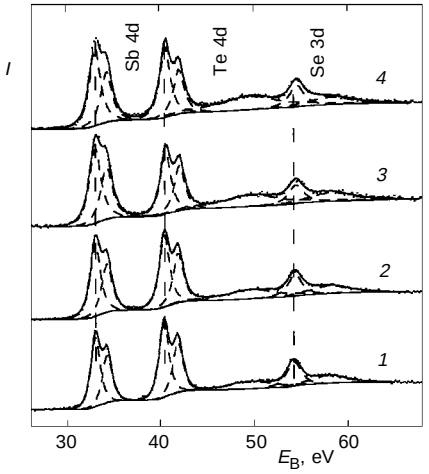

FIG. 5

High-resolution narrow-scan spectra of Sb 4d, Te 4d and Se 3d electrons in Sb_2Te_2Se. (*1*) Clean surface; (*2*) surface sputtered by Ar^+ ions, E = 200 eV, I = 4.4 . 10^{15} ion/cm^2; (*3*) E = 400 eV, I = 3.5 . 10^{16}; (*4*) E = 4 keV, I = 1.1 . 10^{17} ion/cm^2

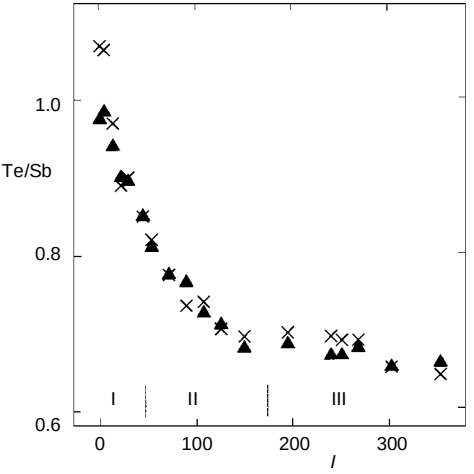

FIG. 6

Dependence of the Te/Sb atomic ratio on ion dose, I (. 10^{14} ion/cm^2), in Sb_2Te_2Se. (I) E = 200 eV, (II) E = 300 eV, (III) E = 400 eV; ▲ θ = 45°, × θ = 5°

structure of the sample is damaged at ion doses $I > 20 \cdot 10^{14}$ ion/cm^2 and as a result the value of the Te/Sb atomic ratio does not depend on the detection angle. On the other hand the Se/Sb ratio (Fig. 7) measured at 5° is always higher than that measured at 45°, indicating the surface segregation of selenium. It is interesting that the sputtering with low ion energies (E = 300 ± 100 eV) caused greater changes in surface stoichiometry than sputtering by ions with energy in keV range at comparable ion doses (see Table IV).

TABLE IV
Surface composition (at.%) of the Sb_2Te_2Se sample before and after Ar^+ ion sputtering (E = 200 ÷ 400 eV) obtained at two different detection angles

Ion dose	5°			45°		
	Sb	Te	Se	Sb	Te	Se
0	40.1	42.9	17.8	41.0	40.6	18.4
4.5	41.0	39.8	19.2	42.7	40.2	17.1
350	51.4	33.2	15.4	52.2	34.5	13.3
1 120[a]	47.1	36.0	16.9	50.0	36.0	14.0

[a] E = 4 keV.

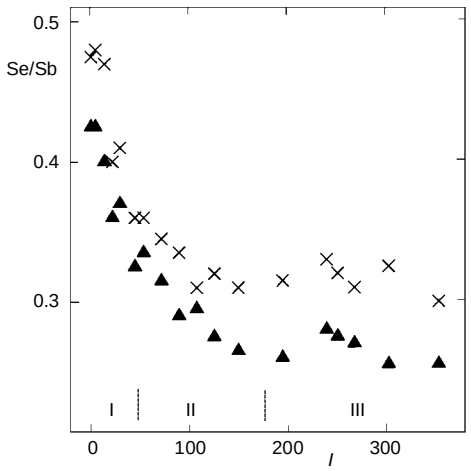

FIG. 7
Dependence of the Se/Sb atomic ratio on ion dose, I, in Sb_2Te_2Se. Definitions as in Fig. 6

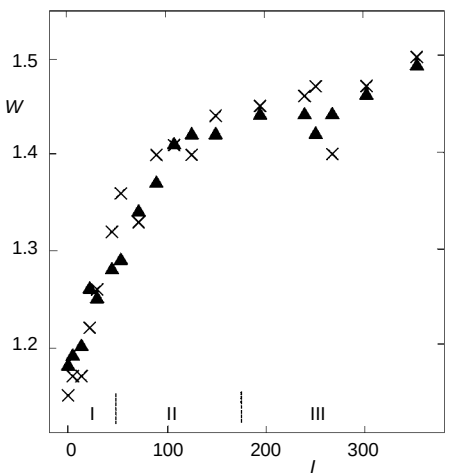

FIG. 8
Full width at half maximum of Sb N_5 line, W (eV), *versus* ion dose, I, for Sb_2Te_2Se. Definitions as in Fig. 6

With increasing ion dose the widths of the core level spectra increase. This increase is best measured with narrow and intense Sb 4d lines (Fig. 8) and it can be attributed to the presence of several chemical states of Sb atoms in the sputtered surfaces. It should be mentioned that for ion doses up to 20 . 10^{14} ion/cm^2 the width of the Sb 4d line does not change. The change in the chemical environment of Sb atoms induced by ion sputtering is also reflected in changes of the core level binding energies. The almost linear increase in separation, ΔE, of Se 3d and Sb $4d_{5/2}$ levels (Fig. 9) is mainly due to the decrease of Sb $4d_{5/2}$ binding energy, indicating that Sb atoms are less positively charged in the layer damaged by ion bombardment. This behaviour is quite consistent with observed decrease of concentration of the negatively charged Te and Se atoms in the sputtered surfaces.

In Fig. 10 typical core level spectra of virgin and sputtered surfaces of $(Bi_{0.7}Sb_{0.3})_2Se_3$ (111) sample are presented. The sputtering results in surface enrichment by Bi (Fig. 11 and Table V), which is proportional to ion dose. In contrast to Sb_2Te_2Se sample the saturation is achieved at ion doses as high as $I > 1$. 10^{17} ion/cm^2. The concentration of Sb does not change during sputtering. New chemical states of Bi are created during sputtering leading to the broadening of the Bi $5d_{5/2}$ line (Fig. 12). The separation between the Se 3d and Bi $5d_{5/2}$ lines increases with increasing Bi/Se ratio (Fig. 13). The Bi $5d_{5/2}$ spectra of the sputtered sample can be fitted by two overlapping lines (Fig. 14) separated by 0.8 eV and corresponding to metallic Bi and Bi atoms in

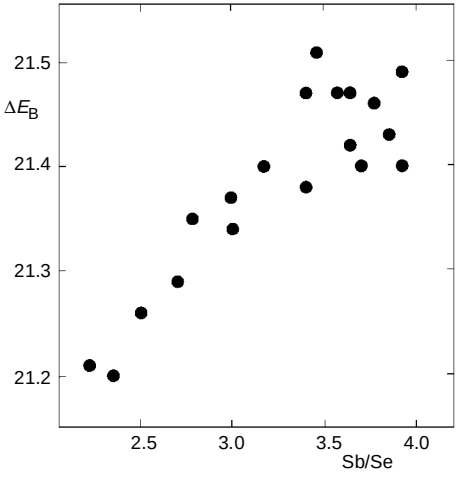

FIG. 9

Energy separation, ΔE (eV), between Se 3d and Sb $4d_{5/2}$ binding energies in dependence on Sb/Se atomic ratio for Sb_2Te_2Se sample bombarded by Ar ions

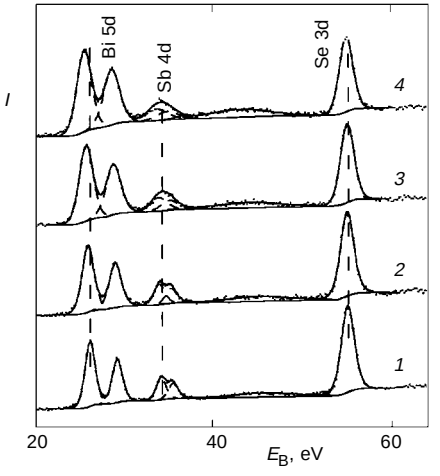

FIG. 10

High-resolution narrow-scan spectra of Bi 5d, Sb 4d, and Se 3d electrons in $(Bi_{0.7}Sb_{0.3})_2Se_3$. (*1*) Clean surface; (*2*) surface sputtered by Ar^+ ions, E = 300 eV, I = 6.4 . 10^{15} ion/cm^2; (*3*) E = 3 keV, I = 1.8 . 10^{16}; (*4*) E = 9 eV, I = 1.5 . 10^{16} ion/cm^2

selenide. The intensity of the peak corresponding to metallic state increases with increasing ion dose.

The sputtering of multicomponent samples is a rather complicated process and many different mechanisms, comprising implantation of primary ions, relocation of sample atoms (atomic mixing), amorphization, enhanced diffusion and surface segregation as

TABLE V
Surface composition (at.%) of the $(Bi_{0.7}Sb_{0.3})_2Se_3$ sample before and after Ar^+ ion sputtering (E = 200 ÷ 400 eV) obtained at two different detection angles

Ion dose	5°			45°		
	Bi	Sb	Se	Bi	Sb	Se
0	36.7	12.4	50.9	38.4	12.1	49.5
4.5	38.7	11.3	50.0	39.7	11.5	48.8
90	44.5	12.9	42.6	44.9	12.2	42.9
4 700[a]	52.7	12.7	34.6	53.6	11.0	35.4

[a] E = 5 keV.

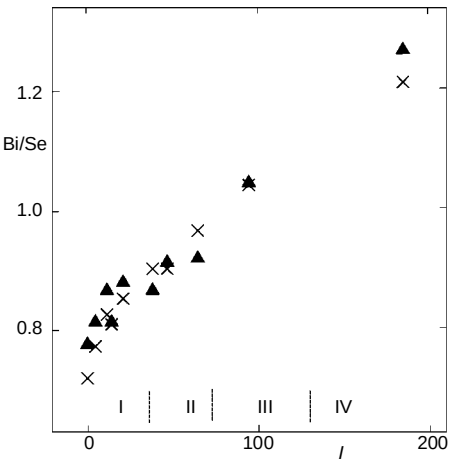

FIG. 11
Dependence of the Bi/Se atomic ratio on ion dose, I (. 10^{14} ion/cm^2), in $(Bi_{0.7}Sb_{0.3})_2Se_3$. (I) E = 200 eV, (II) E = 300 eV, (III) E = 400 eV, (IV) E = 3 keV; ▲ θ = 45°, × θ = 5°

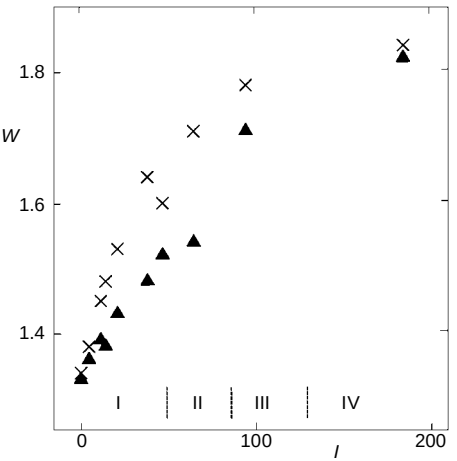

FIG. 12
Full width at half maximum of Bi O_5 line, W (eV), *versus* ion dose, I, in $(Bi_{0.7}Sb_{0.3})_2Se_3$. Definitions as in Fig. 11

well as preferential sputtering. All these effects may lead to enrichment or depletion of the surface in one of the components. The most important is the preferential sputtering which stems from the different atomic sputtering yields. If the sputtering yield of the sample components does not depend on their bulk concentration the surface concentration of a given component is inversely proportional to its sputtering yield and the surface is enriched in the element with lower sputtering yield. For two components we have:

$$C_A^s/C_B^s = (Y_B/Y_A)\,(C_A^b/C_B^b) \quad , \qquad (1)$$

where the subscripts A and B denote the two components and superscripts and b refer respectively to surface and bulk.

According to linear collision-cascade theory[13] the ratio of the sputtering yields of the two target components, A and B, Y_A/Y_B is defined only by the masses M_A and M_B and the surface binding energies E_A and E_B, being given by:

$$Y_A/Y_B = (M_B/M_A)^{2m}\,(E_B/E_A)^{1-2m} \quad , \qquad (2)$$

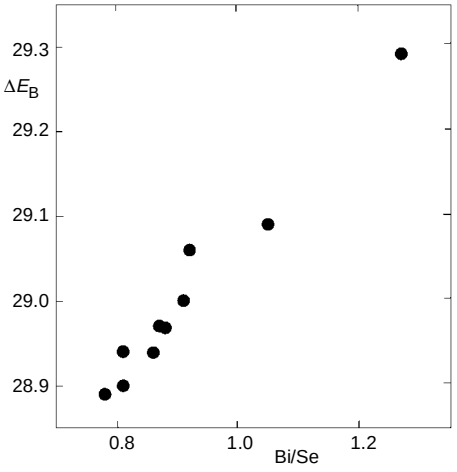

FIG. 13
Energy separation, ΔE (eV), between Se 3d and Bi $5d_{5/2}$ binding energies in dependence on Bi/Se atomic ratio for $(Bi_{0.7}Sb_{0.3})_2Se_3$ sample bombarded by Ar ions

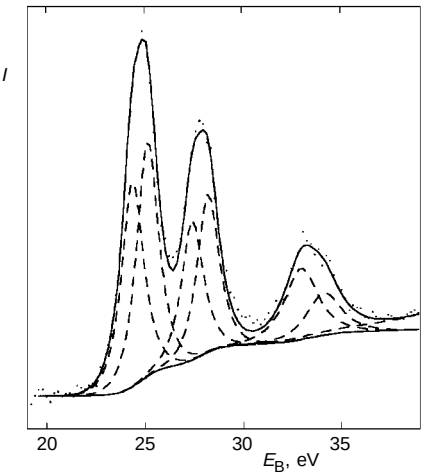

FIG. 14
Fitted photoelectron spectra of Bi 5d and Sb 4d electrons for $(Bi_{0.7}Sb_{0.3})_2Se_3$ sample sputtered by Ar^+ ions, $I = 14 \cdot 10^{14}$ ion/cm^2

where relevant values of the parameter m should be in the range $0 \leq m \leq 0.25$, depending on the ion energy and masses M_i.

Within the linear cascade regime the theory therefore predicts preferential sputtering to depend only on the mass and surface binding energy differences of the components involved and on the magnitude of the parameter m. Let us to mention that the above results were derived for an homogeneous medium but their validity is not limited to this situation. In the case of inhomogeneous samples they can be generalized by using average compositions over relevant depth ranges. According to this model the preferential sputtering of lighter component and therefore surface enrichment in the heavier one should occur. However, since m is small, more important are usually differences in surface binding energies resulting in preferential removal of the more weakly bound atoms.

In Table VI the masses and surface energies of the pertinent elements are given. (In agreement with ref.[23] we assumed that the elemental surface energies equal to their sublimation energies[24].) These data lead to the following sequence of the sputtering yields $Y_{Bi} < Y_{Sb} < Y_{Te} \approx Y_{Se}$. The low sputtering yield of Bi is mainly determined by high atomic mass while differences between remaining elements are caused by different surface binding energies. The measured changes of surface composition of the samples achieved at higher ion doses are thus in qualitative agreement with expectations based on linear cascade model.

CONCLUSIONS

X-Ray photoelectron spectroscopy was applied for evaluation of the changes of atomic charges caused by substitution of Te by Se in Sb_2Te_3 and Bi by Sb in Bi_2Se_3. The core level binding energies in Sb and Te increased by 0.3 eV on substitution, showing that the positive charge on Sb and the ionicity of bonding in the crystal increases. On the other hand the atomic charges in Bi_2Se_3 did not change on substitution. The surface composition of Sb_2Te_3 and Sb_2Te_2Se (111) surface calculated from the XPS data was in

TABLE VI
Atomic masses, M, and sublimation heats (kJ/g-atom) at 298 K

Atomic no.	Element	M	ΔH_s^{298}
34	Se	78.96	206.8
51	Sb	121.75	262.1
52	Te	127.6	195.1
83	Bi	208.98	209.1

agreement with the bulk stoichiometry of the samples while an excess of Bi was observed for Bi_2Se_3 and $(Bi_{0.7}Sb_{0.3})_2Se_{3.0}$ (111) surfaces.

The changes of the surface composition caused by Ar^+ ion bombardment of Sb_2Te_2Se and $(Bi_{0.7}Sb_{0.3})_2Se_{3.0}$ (111) surfaces were measured. The results show that the surface layer probed by the XPS technique (few nm) becomes damaged by atomic mixing and/or amorphization at ion energies as low as 200 eV and at ion doses $I > 2 \cdot 10^{15}$ ion/cm^2. The surface enrichment in Sb (Sb_2Te_2Se) and Bi ($(Bi_{0.7}Sb_{0.3})_2Se_{3.0}$) was observed. The observed changes in surface composition produced by Ar^+ ion sputtering can be interpreted in terms of preferential sputtering of element with high sputtering yields and are in qualitative agreement with results expected from the linear cascade model.

This work was supported by the Grant Agency of the Czech Republic through grant No. 202/95/0042. We wish to express our thanks to Prof. P. Lostak for providing the crystals used in this work. We also acknowledge helpful discussions with Prof. J. Horak.

REFERENCES

1. Scherer H., Scherer S. (Eds): *Proc. 2nd European Workshop on Thermoelectrics, Nancy, November 7–8, 1995.*
2. Dönges E.: Z. Anorg. Allg. Chem. *265*, 56 (1951).
3. Gobrecht H., Boeters K.-E., Pantzer G.: Phys. *177*, 68 (1964).
4. Ivlieva V. I., Abrikosov N. Kh.: Dokl. Akad. Nauk SSSR *159*, 1326 (1964).
5. Gobrecht H., Seek S.: Z. Phys. *222*, 93 (1969).
6. Lostak P., Stary Z., Horak J., Pancir J.: Phys. Status Solidi A *115*, 87 (1989).
7. Horak J., Navratil J., Stary Z.: J. Phys. Chem. Solids *8*, 1067 (1992).
8. Horak J., Drasar C., Novotny R., Karamazov S., Lostak P.: Phys. Status Solidi A *149*, 549 (1995).
9. Wada H., Takahashi T., Nishizaka T.: J. Mater. Sci., Lett. *9*, 810 (1990).
10. Corbett J. W.: Surf. Sci. *90*, 205 (1979).
11. Auciello O., Kelly R. (Eds): *Ion Bombardment Modification of Surfaces*. Elsevier, Amsterdam 1984.
12. Pignataro S.: Surf. Interface Anal. *19*, 275 (1992).
13. Behrisch R.: *Topics in Applied Physics*, Vol. 47, Chaps 1 and 2. Springer, Berlin 1981.
14. Benninghoven A, Rüdenauer F. G., Werner H. W.: *Secondary Ion Mass Spectrometry*, Chap. 2. Wiley, New York 1987.
15. Shirley D. A.: Phys. Rev. *85*, 4709 (1972).
16. Hughes A. E., Sexton B. A.: J. Electron Spectrosc. Relat. Phenom. *46*, 31 (1988).
17. Scofield J. H.: J. Electron Spectrosc. Relat. Phenom. *8*, 129 (1976).
18. Debies P., Rabalais J. W.: Chem. Phys. *20*, 277 (1977).
19. Takahashi T., Sagawa T., Hamanaka H.: J. Non-Cryst. Solids *65*, 261 (1984).
20. Wagner C. D. in: *Practicals Surface Analysis* (D. Briggs and M. P. Seah, Eds), Vol. 1, p. 595. Wiley, Chichester, New York 1990.
21. Bastl Z.: Unpublished results.
22. Wagner C. D., Joshi A.: J. Electron Spectrosc. Relat. Phenom. *47*, 283 (1988).
23. Betz G., Wehner G. K. in: *Sputtering by Particle Bombardment* (R. Berisch, Ed.), Vol. II, p. 24. Springer, Berlin 1983.
24. Gschneidner K. A. in: *Solid State Physics* (F. Seitz and D. Turnbull, Eds), Vol. 16, p. 275. Academic Press, New York 1964.